OPERATIONAL PROCESSING OF SATELLITE CLOUD PICTURES BY COMPUTER

C. L. Bristor, W. M. Callicott, and R. E. Bradford

National Environmental Satellite Center, Environmental Science Services Administration, Washington, D.C.

ABSTRACT

This survey paper explains currently applied procedures whereby operational products are formed from digitized satellite cloud pictures. Sufficient details are provided so that prospective users of the products may understand how they are produced. Comments on the outlook for digital product embellishments and augmentations are provided.

1. INTRODUCTION

Experience with digitized TIROS and Nimbus cloud pictures [3, 4, 10, 11] has provided a background for the present automated system for handling video data. Operational procedures which are currently in a beginning stage have evolved essentially as initially projected for Nimbus [5].

Despite the difficulties involved in treating vidicon cameras as meteorological sensors and apart from the fact that cloud photos do not readily provide a substitute for direct probe data, there is nevertheless good justification for providing for automatic extraction of quantitative information from cloud pictures. Apart from the real value of the information, its sheer volume precludes adequate extraction by hand methods. Present nephanalyses generated from typical orbital picture mosaics are expressable in terms of 8- to 10-min. teletypewriter messages—the equivalent of only 30,000 to 50,000 binary bits per mosaic. However the mosaic itself, covering an area 1500 n.mi. wide by 5000 n.mi. long, expressed in digital form at 2-mile resolution with 4-bit brightness elements, amounts to more than 6×10^6 bits. Thus the data bulk is reduced about two orders of magnitude with present hand methods. Although this is probably not a good indicator of information loss, developmental studies over the past several years do suggest that the images contain a far greater quantity of information than is presently being extracted for operational use.

The purpose of this paper is to acquaint the current and potential users of satellite cloud picture data with the computer products which are now becoming operational. The procedure is described for producing full resolution rectified orbital mosaics for direct visual uses, and full resolution rectified multi-pass montages for the generation of meso-scale descriptors. Evolving techniques for machine generated nephanalyses are also discussed along with some ideas for more advanced information extraction. Finally, output products are described—displays and digital forms for further operational and archival use.

2. VIDEO DATA DIGITIZING AND FORMATTING

The first step in the process involves the digitizing of incoming video data which are received via microwave link from the Command and Data Acquisition (CDA) Stations. Much of the specialized equipment originally employed in digitizing Nimbus video data [15] has been used in the present system. However, the presently operational Digital Format System (DFS) has undergone substantial logic changes so that it now operates in some seven different modes [8].

Briefly, in the case of video data from the ESSA–1 satellite, the analog (FM) signals are passed through a discrimination stage so that each raster line appears as a time variable d.c. voltage train. Each such voltage train is sampled repeatedly and converted to a corresponding series of 6-bit digits (bytes). The sample population is adjusted to 500, so that the 500 earth-viewing raster lines produce a 250,000-element square array. In the case of the Advanced Vidicon Camera System (AVCS), used on Nimbus and projected for future ESSA satellites, each 800-line earth-viewing raster is similarly produced as a 640,000-element array.

The sample bytes are packed into 24-bit words and transferred in parallel directly into the memory of a medium scale computer with the aid of certain interface control signals. Additional "interrupt" signals are provided to the computer through synchronizing detectors to arrange the incoming data into "frames" with reference to the beginning of each video raster and with reference to each horizontal raster line within the image. The edited raw digital data are finally produced on magnetic tape ready for further computer processing as described below.

3. DIGITAL RECTIFICATION PROCEDURES

The program for video data ingestion on the Control Data Corporation CDC–924 computer has time available only for a minimum monitoring and conditioning of the

raw sample values. Marker words are added in response to pulses received from the synchronizing detectors and other key format words are also added during the time interval between the acceptance of the digitized video data and the copying of the raw information onto digital video tape. There is need for further conditioning as the data are made available to the large-scale CDC–6600 computer.

First, certain non-earth-viewing samples at the edges must be removed. This is accomplished by a preliminary edge-cropping procedure which produces images containing only earth-viewing samples. The amount of data cropping in a raster row is indicated in an identification word which is inserted as the first word of each retained video raster row. (Plans are projected for the removal of noise bursts and fiducial marks and the interpolative insertion of realistic substitute video information.)

The data are further conditioned by a brightness calibration process. In order to make the individual frames uniform in brightness response, each 16 x 16 raster sample subset is calibrated for gray scale value. The raw video data range in gray scale from 0 to 63. A "zone argument" is determined for each subset and from the proper zone calibration table a replacement gray scale value is selected as a function of the original sample brightness. Thus "normalized" brightness fields are provided for the rectification and analysis programs. The final normalized gray scale values range from 0 to 14. See section 7 for a discussion of calibration effects.

4. RECTIFICATION

The video data are now ready for transformation to arrays oriented to a map projection. The actual rectification process is, in effect, the assignment of raster elements to earth coordinates for replotting. Latitude and longitude values computed for every 32d raster point along every 32d raster row provide an open lattice of earth locations which are used as benchmarks for interpolating the locations of individual raster samples. This lattice was selected because: (a) the computation required for establishing a latitude-longitude value for every point is excessive, (b) the interval between benchmark points approximates a straight line on earth thus minimizing linear interpolation error, and (c) the value 32 is a binary factor permitting computer interpolation shortcuts. Finally, the open lattice latitude-longitude values are converted to map I and J coordinates in a square mesh map overlay. A benchmark table of map I and J values is generated for each video frame processed (reflecting its unique perspective).

5. ORBITAL MOSAICS

The video data are rectified to polar stereographic and Mercator map projections with grid mesh size commensurate with the original resolution. In addition, the polar stereographic array is a binary superset of the commonly

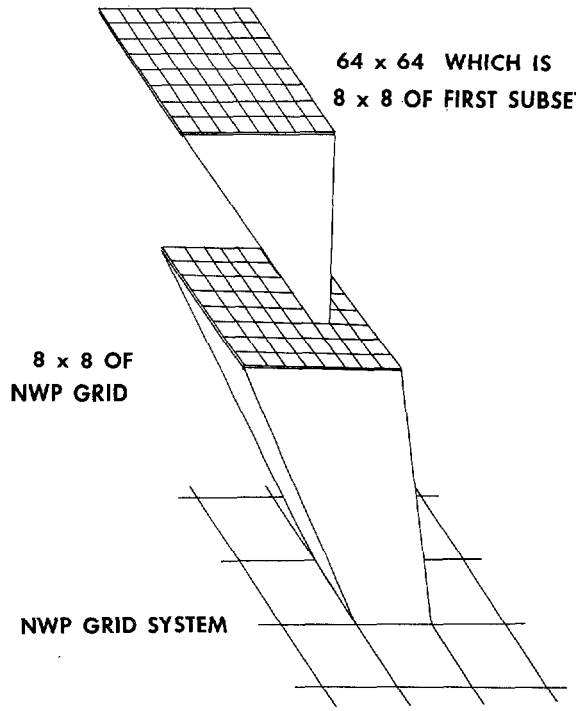

FIGURE 1.—The method is illustrated whereby the NWP mesh is subdivided to obtain a 64 x 64 superset. The two-step breakdown facilitates computer handling.

used numerical weather prediction (NWP) grid system. This array is divided, step-wise, into two sets (see fig. 1). One is an 8×8 set of the NWP system and the other is an 8×8 set of the first thus providing a 64×64 superset. A linear map resolution of approximately 2 n.mi. at the equator and 4 n.mi. at the pole is realized.

The rectification or replotting logic requires memory space for all video data samples within the map array region being viewed. Memory overhead space is required in that image rasters do not generally coincide with rectangular subsets of the mapped array. Video data are stretched or distorted over the array as a function of the map projection mathematics. This stretching is more severe in image areas where foreshortening is evident. Since the complete 64×64 polar array has 4096×4096 grid squares per hemisphere (corner overlap with opposing hemisphere), methods for array storage compaction are required. One might consider output buffer space only for a single picture sequence. However, an orbital swath of data requires a minimum of 2,464,000 grid squares (this minimum case occurs when the picture swath is aligned favorably with the array mesh system). This too exceeds the available high speed computer memory capacity. The polar array grid square area required for a swath is, therefore, broken into parts called subregion arrays. Each subregion is an irregular skew-shaped array containing those grid square "bins" in which imagery is stored. Because the bins are arranged serially in the computer, a two-dimensional indexing scheme is required for random access to the data (see fig. 2). Even so, the

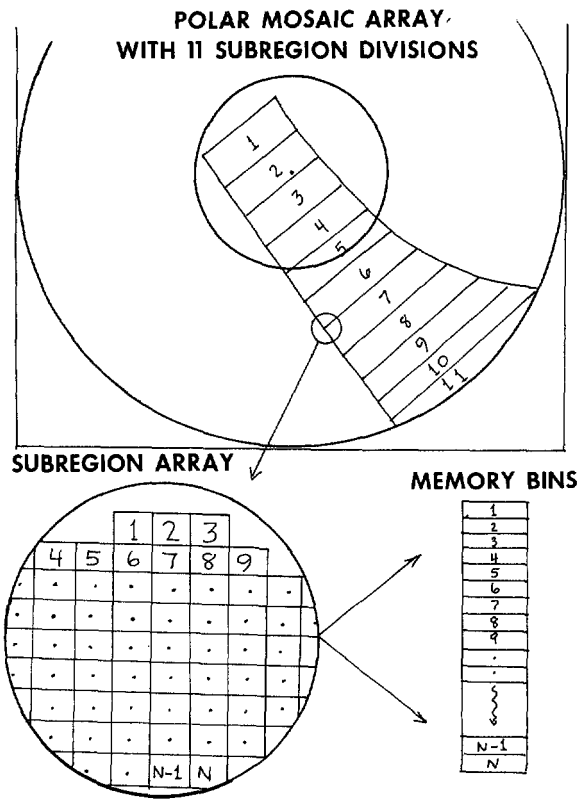

FIGURE 2.—The need for indexing logic is indicated by the sequential storage of skewed data trains.

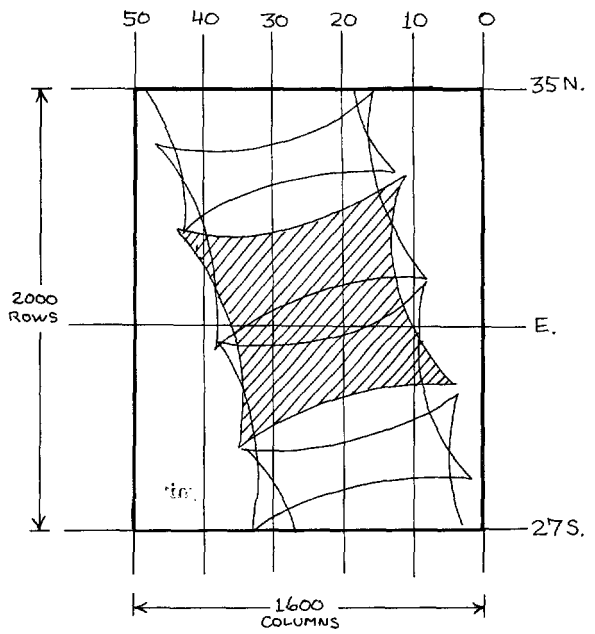

FIGURE 3.—The Mercator mosaic map coverage is indicated (heavy border) along with the data array dimensions.

irregular arrays require memory space for 224,000 samples so that only computers with large-scale memory capacity can be used efficiently for the rectification problem.

The Mercator grid square array contains 32 mesh intervals per degree of longitude. This fixed dimension array consists of 1600 columns and 2000 rows and, when centered about the equator, provides map coverage of approximately 60° of latitude and 50° of longitude. The extreme right hand column is aligned with a meridian selectable in even 5° intervals and the top grid row overlies the top (also selectable) latitude limit (see fig. 3). The indexing problem is not as severe as that for the polar array because the subregions are rectangular.

The extreme volume of grid-square data involved in full resolution rectification stresses the need for efficient programing and for the elimination of redundant processing. In the case of Advanced Vidicon Camera System coverage planned for later ESSA satellites, there is generally considerable frame-to-frame overlap (the amount of overlap is dependent on the picture-taking time interval and the height and inclination of the orbit) and significant overlap between orbital passes—particularly at middle and high latitudes. The data-processing program makes the most efficient use of the computer facilities through machine language coding, and takes advantage of binary (shift) arithmetic and fixed point instructions. The overlap problem is alleviated through the use of internal cropping logic.

The satellite's orbital characteristics and the camera shutter time schedule establish a set of cropping tables which are adjustable to process any desired picture portions. Each frame is cropped uniquely. This permits cropping to minimize sun glint problems and to avoid using imagery having poor brightness response or extreme foreshortening. Central raster lines provide better source imagery from the standpoint of brightness characteristics and resolution, but near the equator where overlap between passes is minimal, the center raster lines contain the sun glint. Where possible (at higher latitudes) sun glint is removed by the use of overlapping imagery (see figs. 4 and 5). Parameters are supplied to the rectification program in a format permitting asymmetric cropping. The cropping facility eliminates processing of data outside the designated area. Minimum redundant processing is allowed in order to guarantee continuity within an orbital swath and to avoid gaps between passes.

Care is taken to eliminate data voids within the mosaic images thereby providing greater eye appeal and guaranteeing continuity for follow-on processing. There are areas in the rectified mosaics where the map resolution exceeds that of the data source. This is particularly true near the equator on the polar array and at higher latitudes on the Mercator array. Since the coarser resolution video samples apply almost as well to adjacent higher resolution map squares, a simple areal average is used to fill voids in the polar array. For convenience the Mercator array is filled by a bi-directional row scan which propagates adjacent values into voids. Both processes create smooth mapped images where voids occur, preserving a continuous picture image. Examples of full resolution orbital mosaics are shown in figures 6 and 7.

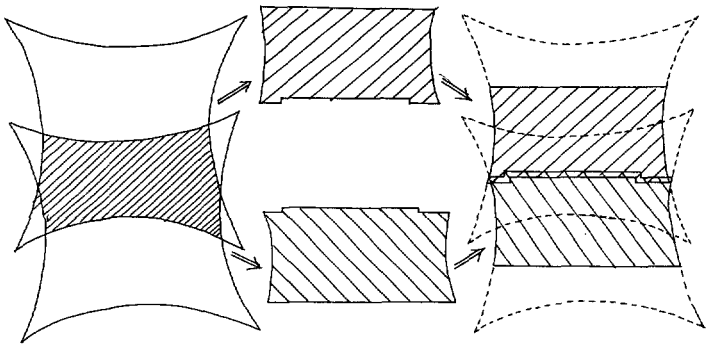

FIGURE 4.—The frame-to-frame overlap permits arbitrary cropping.

6. MONTAGE GENERATION

As the mosaics for adjacent orbital swaths are generated, they are blended into a composite image (montage). Since mosaic arrays are blended in such a way that the most recent data take precedence, a 24-hr. discontinuity occurs at the western edge of the most recent mosaic. Near the poles, where overlap is extreme, imagery is continually being replaced (see fig. 8). Both map montage arrays are maintained in auxiliary memory at all times and neither is purged of information. A continuous coverage product is thereby always available for image extraction or other use.

The polar map array is laid on the map base with the pole in the center and the 80° W. meridian aligned with the lower half of the center column. The Southern

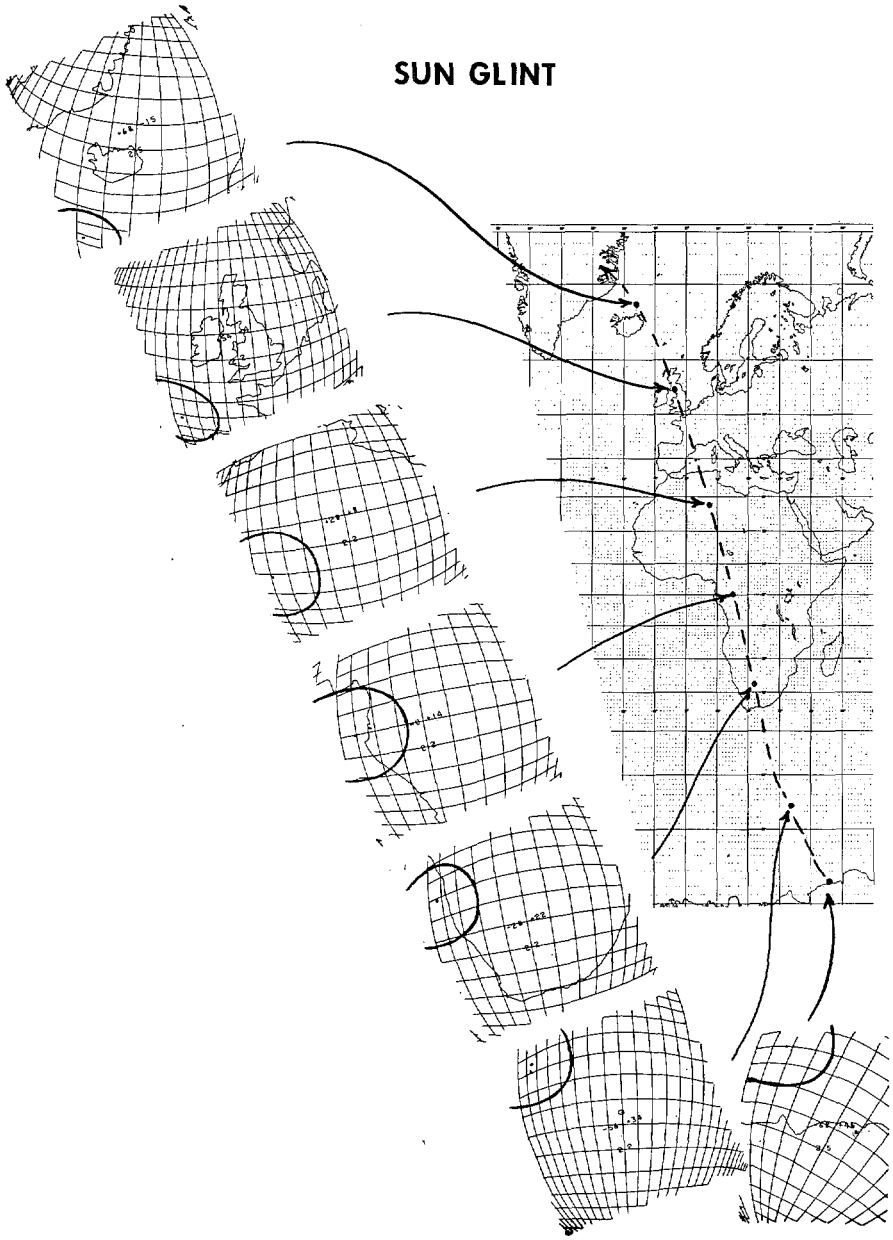

FIGURE 5.—Sample earth *locator* grids are shown as insets on a typical mapped pass for a sun synchronous orbit. It is to be noted that sun glint occurs in all frames.

Hemisphere array is on a like map base except that the 80° W. meridian is the prime upper vertical meridian so that the Southern Hemisphere array is merely an extension of the Northern. Each hemispheric polar montage is a 4096 × 4096 array with the coordinates of the north pole at 2048, 2048 and the coordinates of the south pole at 2048, 6144. The Mercator montage, with a longitude extent of 410° and a latitude coverage from 35° N. to 27° S., has a grid square dimension of 13,120 columns by 2,000 grid rows. The 50° longitude extension precludes splitting an orbital mosaic. The starting position for blending can be selected at any longitude. There is also an image discontinuity at the lateral array boundary limits.

Both arrays are accessible in parts or segments so that one desiring a specific coverage is able to extract only data

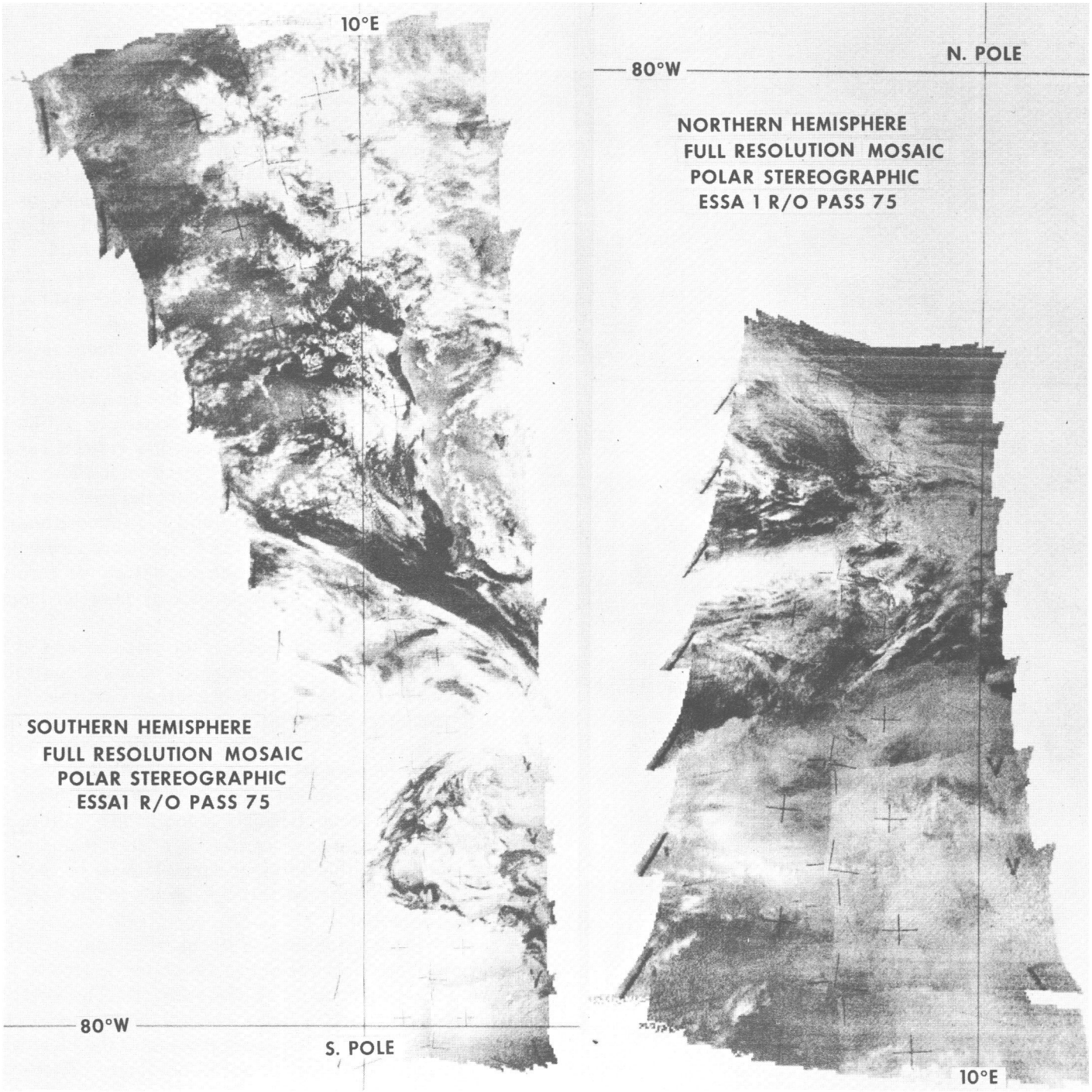

FIGURE 6.—Approximately 40 ESSA 1 pictures are combined into full resolution polar stereographic mosaics. Interpolative filler has been applied where foreshortened imagery has been "stretched" to the map array. Interim brightness calibration utilizing tables from figure 12 has not yet been applied, so "seams" are still apparent in certain overlap areas.

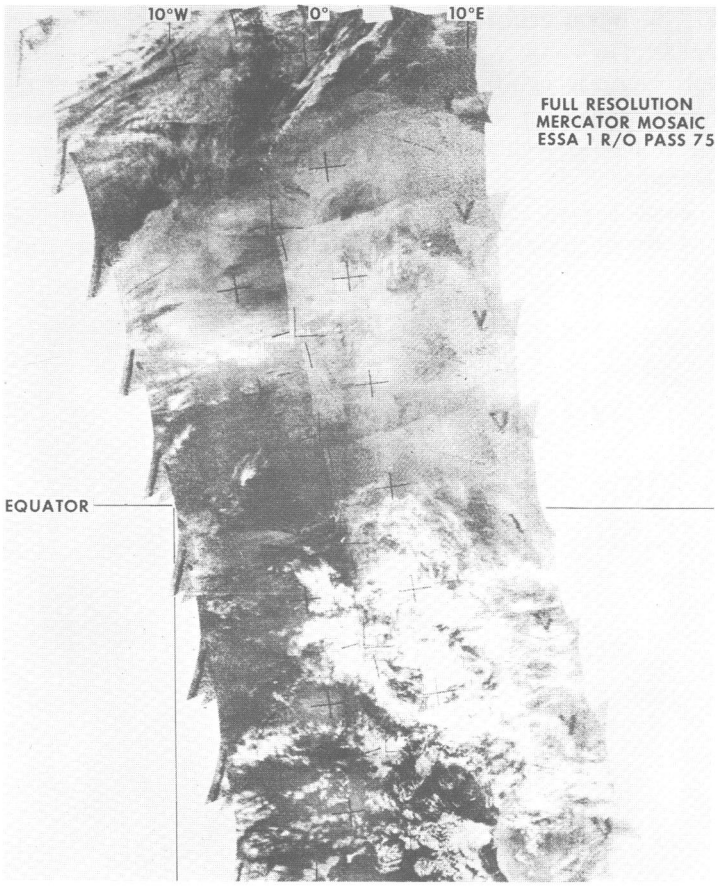

FIGURE 7.—The full resolution Mercator mosaic uses part of the picture sequence shown in figure 6.

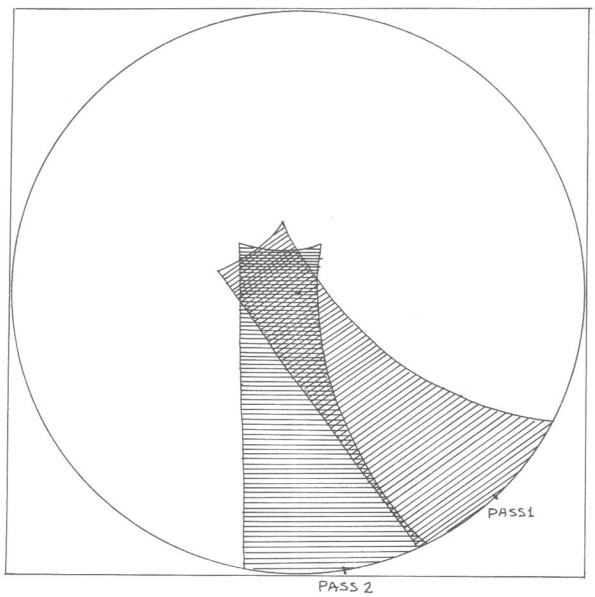

FIGURE 8.—Polar montage. Extreme overlap from pass to pass is indicated by the double shaded area.

in the area of interest. Current products are being projected for operational use on a 6-hourly basis to meet synoptic deadlines (see figs. 9 and 10). Variables which determine map coverage and resolution for the Mercator montage are set by alterable parameters. The polar montage array is bound to the NWP grid square system for compatibility purposes. A total of 830,000 (6-bit byte) computer storage bins is required for the larger segments of this rectification program and about 25 min. are required for processing one orbital picture swath.

7. CALIBRATION EFFECTS

In the description of the rectification process the mechanics of applying brightness calibrations were outlined. The data are altered according to the position in the picture-taking sequence of the frame in which the data reside and the position of the particular sample in the frame itself. The sample position is known only as it is a member of one of the 16×16 sample groups. This knowledge of how calibration is applied is now accompanied by an explanation of the reasons for calibrating and how the calibration function is obtained.

Apart from the cloud-earth scene, vidicon response variations may involve: (a) light transmission differences across the image plane arising from the properties of the optical system of the lens, (b) non-linearities in the x,y raster response pattern arising from the vidicon camera tube and associated electronics, (c) illumination variations due to solar angle (including extreme local sun glint problems), (d) "erase" efficiency and possible contamination from preceding scenes, and (e) time dependent anomalous responses—either response variations during a picture sequence from a single orbital pass or longer-period trends.

Based upon pre-launch calibration pictures and other information [13], item (d) is accepted as an uncontrolled contaminant with a brightness variation contribution of about 5 percent (which could be reduced with an increase in the number of erase scans within the camera exercise cycle). If the camera system can be regarded as a stable sensor package, then one may attempt to compensate for the other listed items through a brightness calibration procedure. (Sun glint, of course, is a very complicated phenomenon but other gradual time changes in the system can likely be detected through trends in the averages of the digital response.)

The most glaring influence of the instrumentation on the data comes from the optical system (filter, aperture, and lens) immediately in front of the vidicon. The aperture controls the amount of light energy impinging on the vidicon face. The filter virtually eliminates the blue light, hence, the light scattered by the atmosphere. These two components are most relevent in determining absolute brightness response. The lens system employed introduces a substantial vignette effect as shown in figure 11. This effect produces a target shaped half tone pattern

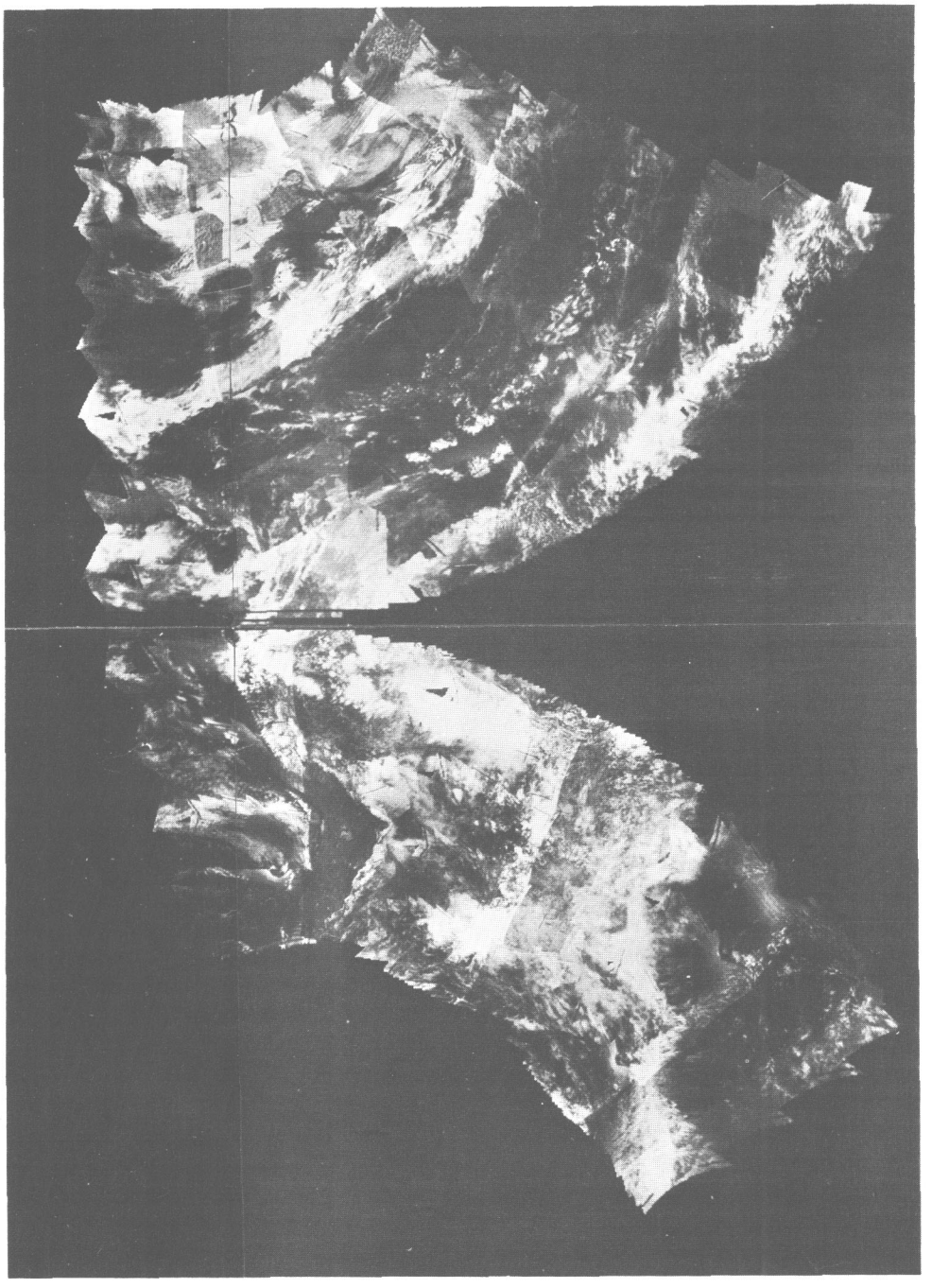

FIGURE 9.—Picture mosaics from adjacent passes are shown in polar stereographic montages. (Upper is Northern Hemisphere, lower is Southern Hemisphere) Reproduction uses a cathode ray film recorder. Latitude-longitude marks have been omitted from this early sample but the vertical seam between film segments is approximately 80° W.

because the digitized data are discrete. Each digital level constitutes a zone. We describe each zone by the fraction (p_i) of the true image brightness presented to the camera system. The inverse of this fraction is the calibration factor for the zone. Two or more camera systems can be "equalized" by establishing the gradient function and maximum p_i for each. The target patterns for the two cameras of ESSA 1 are illustrated in figure 12. The satellite is sun synchronous, assuring constant sun angles to the cameras. Camera 1 is pointed away from the sun and has a larger aperture setting than camera 2 which is pointed toward the sun. Although the biased aperture settings tend to equalize the overall brightness of the images presented to the vidicons, the application of the "target factors" from figure 11 is required to maintain the integrity of the object illumination. The ability to apply such factors efficiently is significantly unique to computer processing. There is thus a facility for linearizing the dynamic gray scale range which is not fully realized in conventional photo processing.

Individual pictures so adjusted are merged into an orbital mosaic as a homogeneous image. Merging

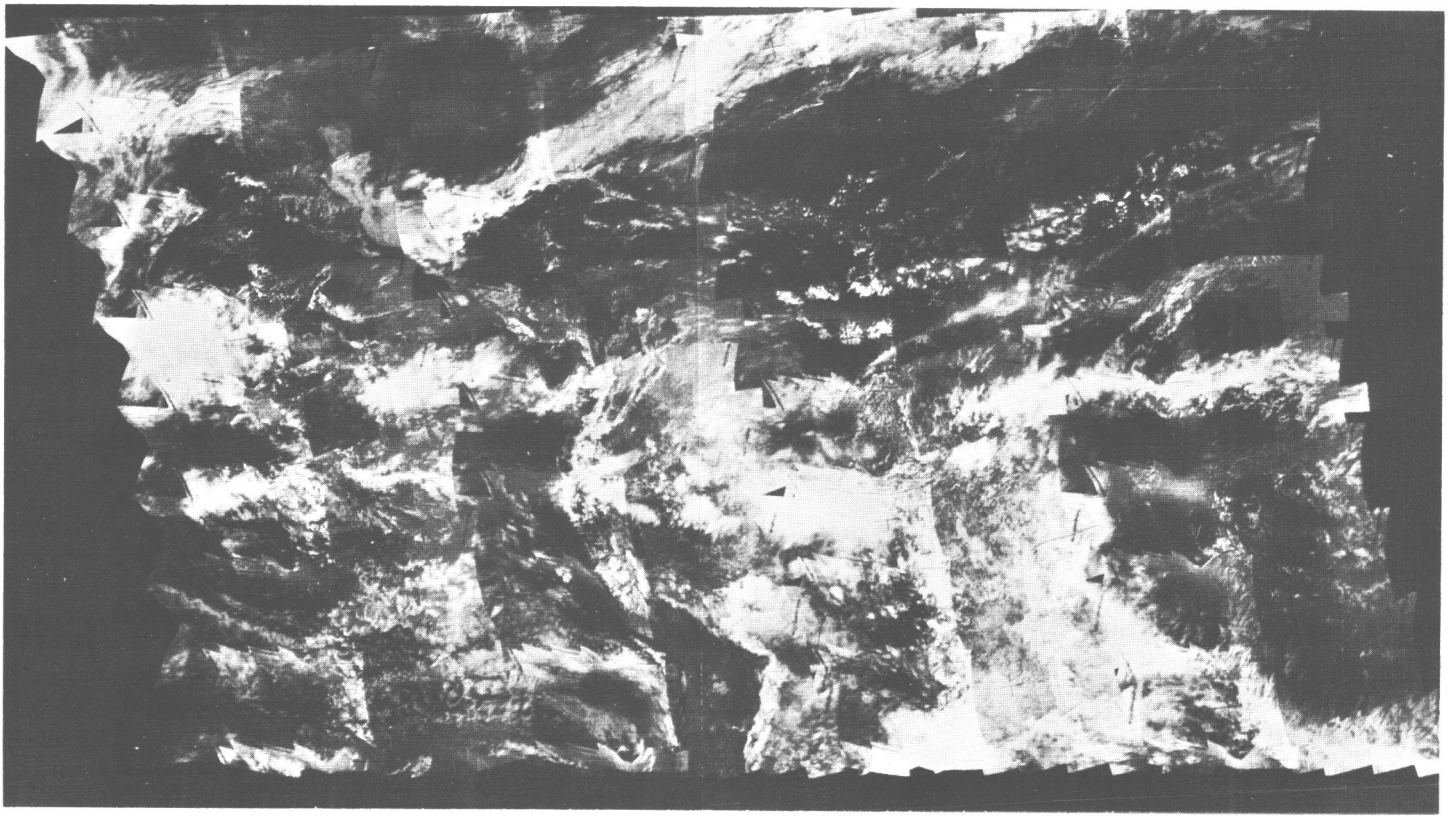

FIGURE 10.—Adjacent mosaics have been combined into a multi-pass Mercator montage similar to figure 9. Early versions of the brightness calibration tables have been used in both figures.

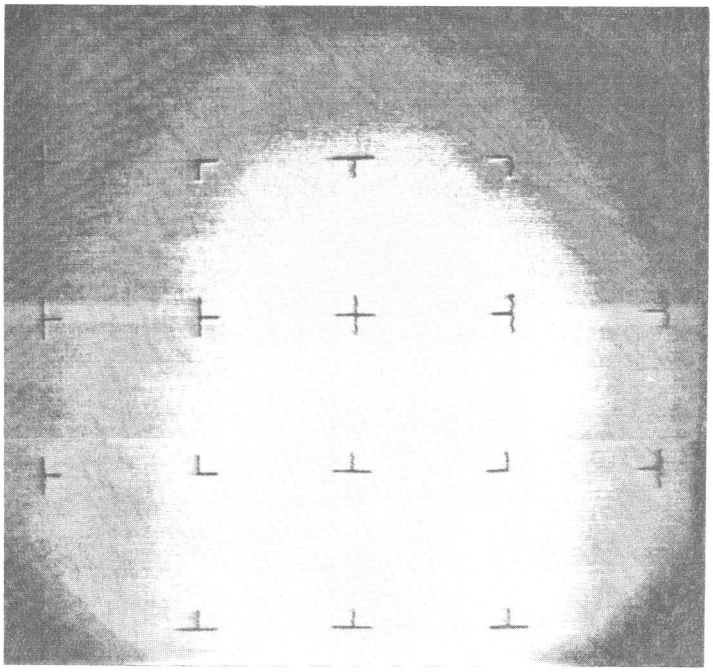

FIGURE 11.—A digital reproduction of a picture of a uniformly illuminated screen taken by the camera (AVSC) of the ESSA 3 prototype is shown. Although the screen illumination was maximum white, the camera response at the corners was near zero, showing the severity of the vignette effect.

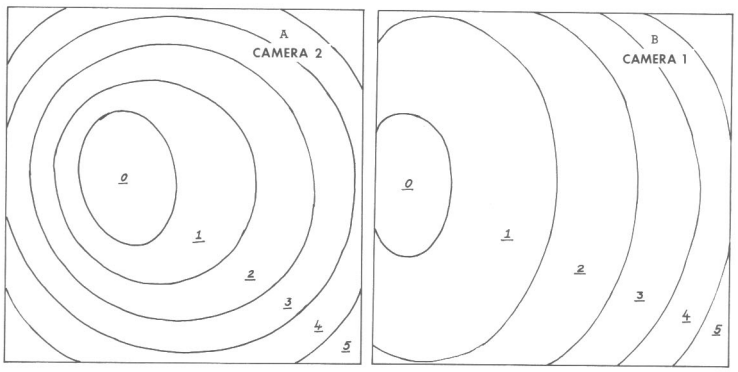

FIGURE 12.—The calibration zones are shown graphically for the two ESSA 1 cameras. (A) Camera 2 points toward the sun and (B) camera 1 points away from the sun. The vignette effect is obvious. The shift of the centers of the patterns (zone zero) to the left demonstrates the influence of the sun's position which is to the left with respect to the figures. Zone zero is the area of maximum response, hence, least adjustment. As the zone number (index) increases the amount of calibration adjustment increases.

mosaics into a montage poses the peculiar problem of accounting for the difference between illumination patterns. The light energy flux at or near the earth's surface is a function only of the angle of incidence of the light ray (disregarding atmospheric refraction, absorption, and scattering). This means that there is a flux discontinuity where mosaics join. The flux is equalized among the mosaics by employing the inverse of the solar incident angle function as a factor. This alteration of the observed images must be considered when the data are examined. There are two major ramifications of this illumination normalization: (a) the angle of incidence is unchanged, leaving (in fact enhancing) the original shadows, and (b) such physical measures as albedo must be considered "normalized" by rendering the flux constant throughout. The original scene is recoverable through knowledge of the illumination patterns and the method of merging the mosaics.

Current ESSA satellites, being sun synchronous, have constant illumination patterns which, when combined with the vignette patterns, provide frame calibration patterns that are dependent on latitude. By means of a standard set of zone tables according to the latitude of the center point of the picture, both calibrations are applied at the same time. The "latitudes" of the reference array tables change with the seasonal position of the sun with respect to the earth's latitude-longitude system.

Although the calibrating scheme has been discussed conceptually, the actual calibration tables are determined empirically. This technique automatically includes compensation for time dependent anomalous response. The structuring of the zone tables permits calibration for any empirically determined nonlinearities. The full details are discussed in another paper [1].

8. DESCRIPTORS AND A NEPHANALYSIS TECHNIQUE

One may consider the picture source information in three categories: the cloud field and its implied dynamically related variables, the earth's surface, and the combined view. Since the clouds tend to dominate the pictures, their isolation and objective description have been the primary goal to date. In view of the practical utility of the present manually produced nephanalyses, current efforts are directed toward the production of an equivalent analysis by automatic means. This effort has led to examining the digitized data for determination of cloud cover and cloud type, the two basic ingredients of the current hand product. The full results of this examination are given in another paper [2]. Essentially it was discovered that a crude estimate of the cloud cover and cloud brightness could be obtained from the difference between the observed brightness and the expected clear air brightness (the background or earth's surface). A more refined estimate is obtained by averaging over some small (mesoscale) areas. An 8×8 cluster of the full resolution montage image data is a convenient group. The cloud cover amount is derived directly by a simple regression technique.

The cloud type is more problematical. The cloud brightness (measure reflectivity) of gives only a partial description of the physical structure of the clouds in these 8×8 groups. It follows that we must have some measure of the geometrical structure in order to adequately characterize the clouds. For this reason we employ what is called the disjunctive index, a measure of the geometrical variability of the clouds in these mesoscale areas. The cloud brightness and disjunctive index combine to give the first estimate of the cloud type. The derived cloud cover and cloud types constitute the basis for a cloud classification. Since no known systems employ reflectivity as a classification property, the relationship of this to conventional systems is not obvious. Thus, whereas manual processing seems to provide good estimates in terms of the standard cloud code, use of the machine product may require new user understanding.

Figure 13 shows the meso-scale cloud estimates for the montage in figure 9. Figures 14, 15, and 16 show close-ups of a small region for cloud cover, cloud brightness, and disjunctive index, respectively, to permit closer study of the numbers computed. Even the meso-scale descriptors provide data in a volume which is impractical to use manually and which is unnecessary for most macro-scale computer applications. Whereas straightforward areal averages centered on NWP grid points might suffice in the latter case, conventional nephanalyses require summarization into homogeneous subfield regions. A problem arises in subfield separation in that the fields requiring analysis are not smoothly varying, like the conventional pressure map topographies, but are discrete. Since the subfields may be regarded as plateaus with shoulder discontinuities, edge detection logic is employed. The Laplacian is a well known edge detector which is used with certain discriminant categories to provide subfield separation boundaries. In practice the x and y components of the Laplacian are used separately to obtain edges and subfield averages in two directions. The combination of these averaged fields provides the contoured nephanalysis for display.

9. OUTLOOK FOR ADVANCED INFORMATION EXTRACTION

Apart from visual summarization products, the averaged cloud cover and cloud type fields are retained at meso-scale resolution along with the original meso-scale descriptors. The meso fields can now be used individually or in combined form in the computer with sufficient hypotheses to provide the users with other desirable information. The meaning of the information depends upon the needs of the user and his interpretation of the data. The above summary nephanalysis describes the state of the clouds without portraying any of the implications of their configurations. Research is showing that there are at least semi-quantitative relationships between some cloud forms

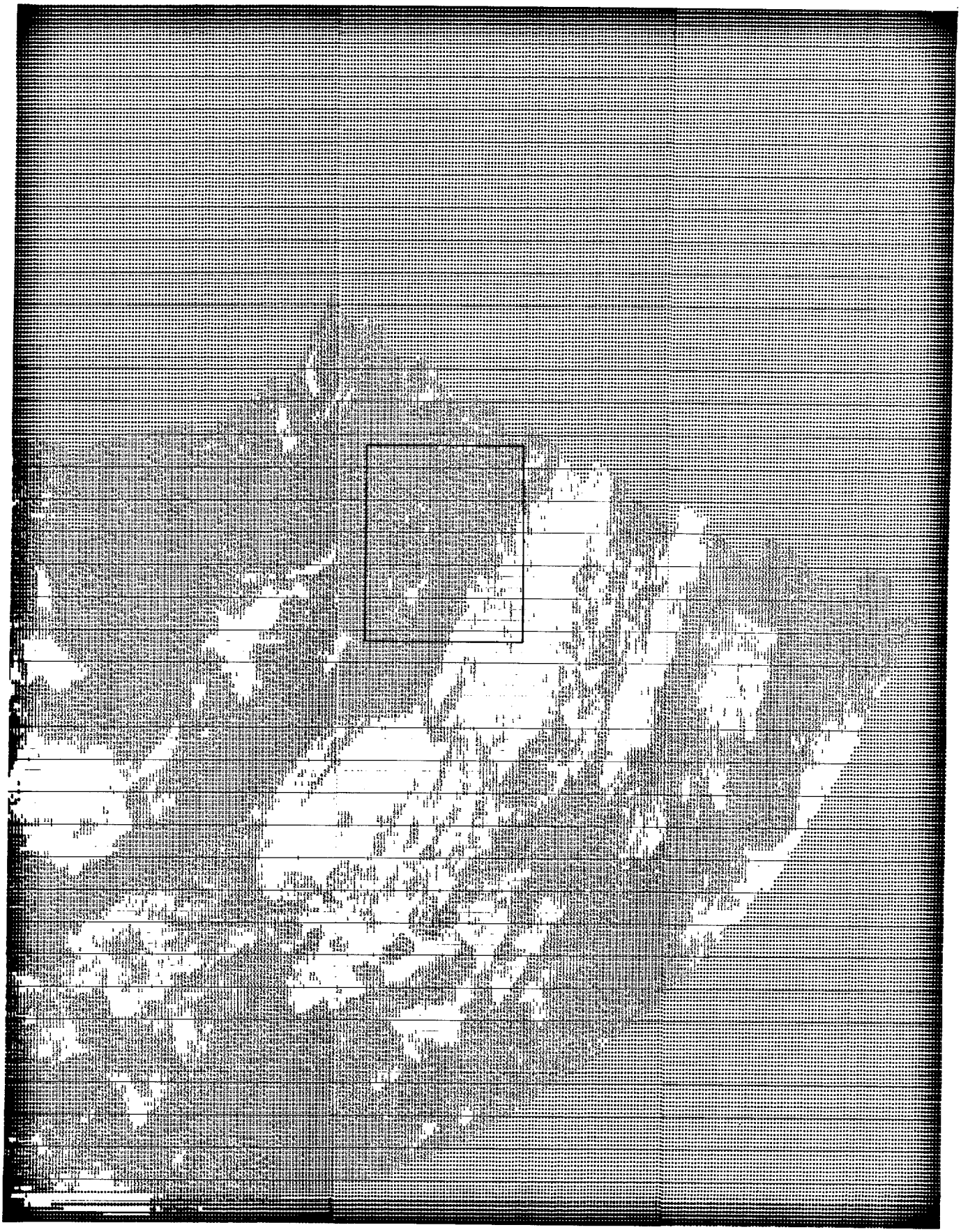

FIGURE 13.—The broad features of the clouds in figure 9 are shown at meso-scale resolution. Blank areas indicate clear. Each printed digit represents the cloud cover in an 8 × 8 sample cluster.

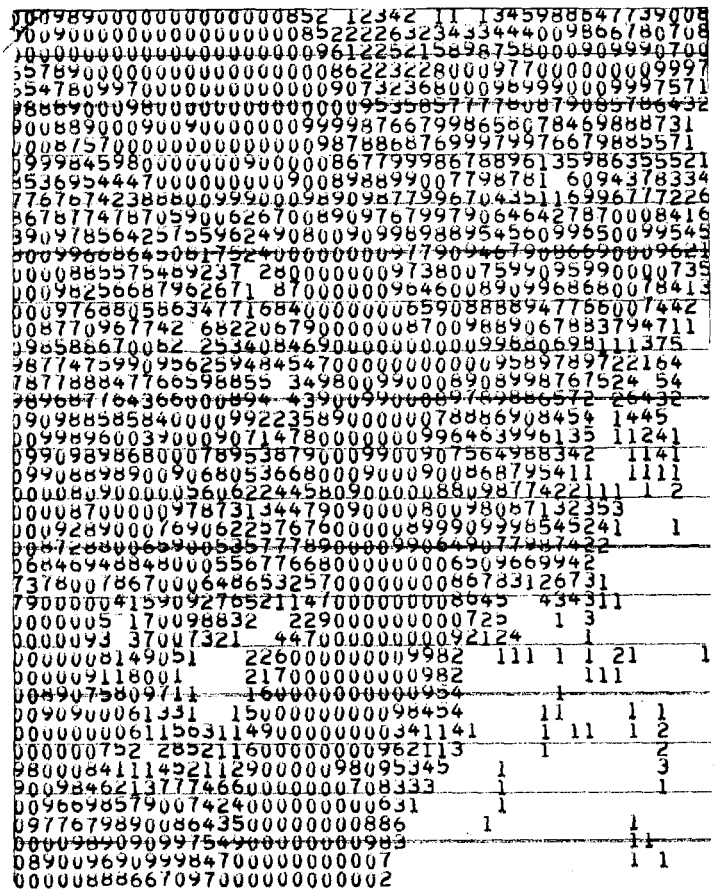

FIGURE 14.—Cloud cover in expanded form is shown for the inset area of figure 13. Zero indicates ten tenths, 9 is nine tenths, etc.

Right above.

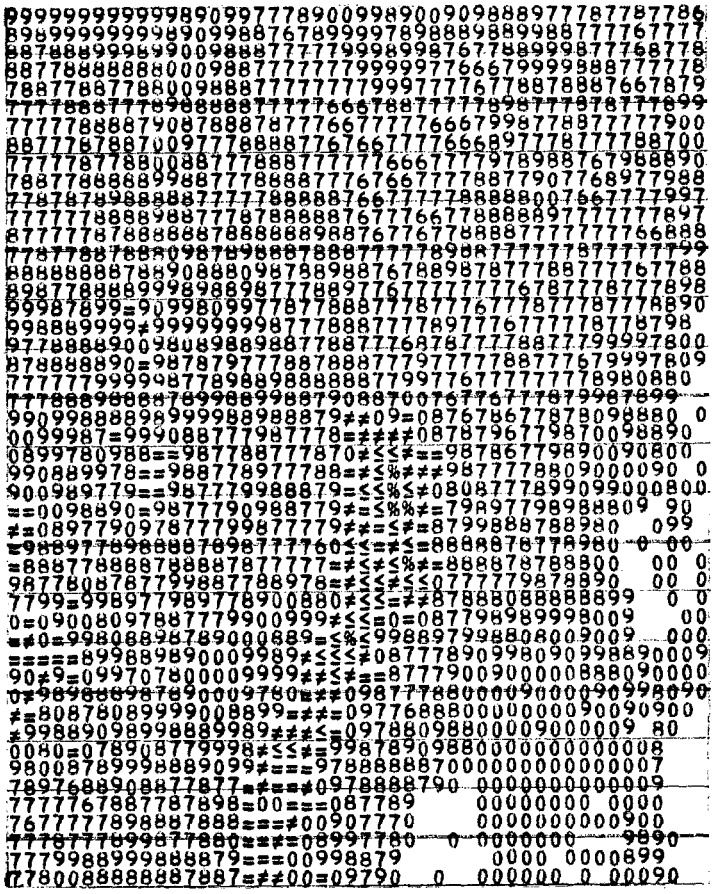

FIGURE 15.—The mesoscale cloud brightness estimates are shown for the same region as in figure 14. Blank areas indicate that no clouds at all were detected. A brightness estimate is given even if only one of the 64 bins was determined to have clouds. Thus areas having less than ½ of $\frac{1}{10}$ cloud cover will be clear in the cloud cover chart but may not be clear in the brightness chart. The numerical equivalents for the printed characters are: %, 14; ≤, 13; ≠, 12; =, 11; 0, 10; 9, 9; etc.

Right.

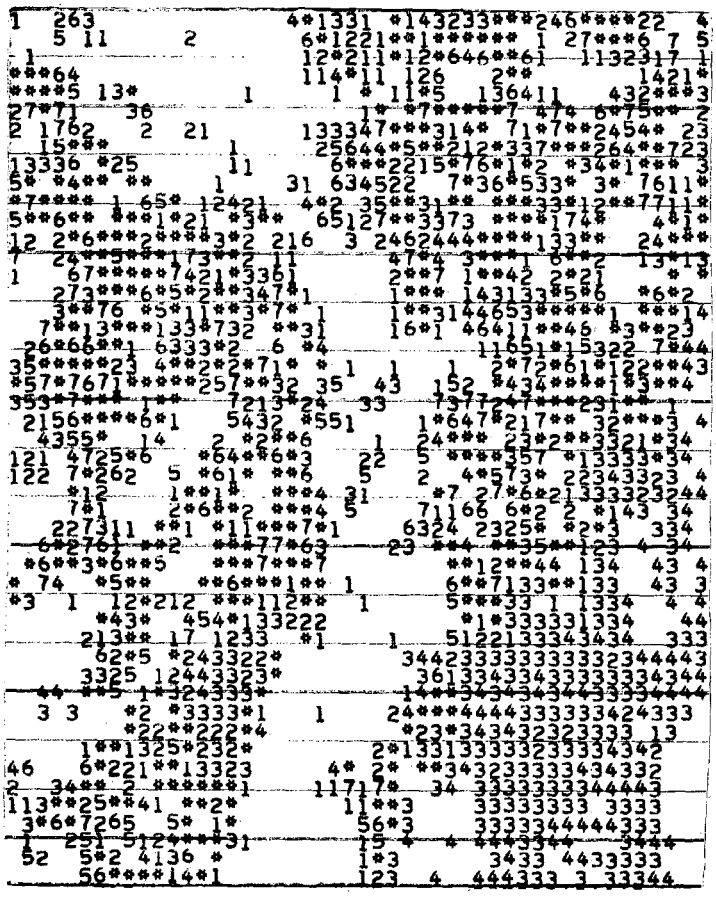

FIGURE 16.—A disjunctive index related to the variance of cloud cover is shown for the same region as that in figure 14. Although the computation and representation schemes are too complex for short description, it is clear that there is an association between low disjunction (blank) and cloud cover uniformity.

and certain dynamic variables. Objective rules arising from such relationships can be applied to calculate estimates of the dynamic variables.

A sizable list of likely relationships has evolved as the result of numerous studies made since the launching of TIROS I. To some researchers a most appealing relationship has been that between clouds and vertical motion. Unfortunately no outstanding quantitative application has come about although statistical estimates have been used with some success [12]. Perhaps one of the major problems is that the absence of clouds cannot give any estimate of the vertical motion. For this reason it seems that clouds can be only a partial predictor of the vertical motion field. Since clouds are also integral manifestations, their use in a three-dimensional trajectory cloud analysis and forecasting technique is more appealing [9]. Recently there has been active interest in perhaps the most natural variable to consider, the moisture field. Although there is not a great amount of evidence, there are indications that reasonable estimates of moisture concentration in the lower and middle troposphere may be made from cloud field information [14].

Beyond the meso-scale descriptors mentioned thus far, there are, of course, other possibilities at the macro- or micro-scale levels. Spatial functions of meso parameters already described are one possibility, since it seems likely that cloud features described by local descriptors may be additionally categorized with reference to their relative position within the broadscale system. Thus the shortest distance to (or direction of) imagery having different meso characteristics may serve as added macro descriptors. There is also great challenge in extracting additional shape, size, orientation, and curvature information from the full resolution source montage. Experiments in extracting streakiness and orientation parameters from rectified Nimbus I high resolution radiometer imagery indicate the feasibility of such efforts. Such descriptors permit one to consider extraction of added meteorological information from the imagery. For example, wind information at high cloud levels might be automatically extracted through descriptors which deal with cirrus streamers emanating from tops of thunderstorms cells. Streamer length-to-width ratios may relate to wind speed, and wind direction could likely be deduced by noting the streamer direction and noting which end was characterized by the sharper brightness gradient (the upwind end). Measurement of wavelength and orientation of wave clouds near mountain barriers, as a means of obtaining information concerning the mean wind in such regions [6], also appears feasible through automatic information extraction techniques.

Finally mention should be made of the opportunities for making various types of climatological summaries based upon the rectified digital video data in a variety of resolution scales. By screening only the brightest responses in the global high resolution montage, one could, for example, obtain a cloud summarization for five days or a month by which storm tracks and the semipermanent centers of action would be conveniently revealed.

Although there has been no definitive progress in deriving dynamic variables, all investigations have, to one degree or another, supported the hypothesis that the cloud distributions reflect, to some extent, the properties of the processes in the atmosphere of which they are a part. For this reason, it is important that objective cloud field description capability be provided so as to permit the development of procedures whereby video data may be converted into representations of information that would otherwise require direct probe observation.

10. OUTPUT PRODUCTS

Preceding illustrations provide samples of the available output products. Figures 7 and 8 were produced on a standard weather facsimile recorder. Input signals are generated by means of a digital-to-analog encoder which accepts information from the computer produced magnetic tape. Three-bit bytes provide gray-scale information for 1710 locations on each facsimile raster line. The montages shown in figures 10 and 11 were produced on a specialized cathode ray microfilm recorder [7]. Digitized images are expressable on a 0–15 gray scale within a 1024×1024 or (optional) 2048×2048 matrix. Legends and other annotation are produced by built-in character and line generators. Apart from visual products, digital information is available on an operational basis for possible additional specialized computer treatment or for reformatting to fit other visual display devices. At present this information is available at meso-scale resolution (percent cloud cover, disjunctive index, etc.) on magnetic tape for local use and possible point-to-point transmission. Each file consists of a series of 17,280-bit records (divisble by 12, 24, 36, 48, and 60) written in standard binary format. The first record contains a variety of documentation items including date, time, satellite identification, map projection and I, J data array boundaries. The remaining records contain packed meso-scale descriptor data expressed in three- and four-bit bytes. Each data string is labeled in terms of J row, starting I column, and total meso-mesh (8×8) population for that row. The exact message content will likely remain fluid until stabilized through proven usage.

Daily global mapped imagery is available on disk in two polar arrays and an overlapping Mercator array. This material is archived daily on three magnetic tapes and is available from the archive for further study. The raw digitized video tapes are retained for a limited period (about a week) and are then returned for re-use.

11. SUMMARY REMARKS

Satellite picture data processing by computer has been started in what is considered to be a practical real time operation. Flexibility has been the watchword in the logical design of the programing effort. The system is

thereby relatively insensitive to superficial differences in image source data and may easily be modified as developments in output products dictate. The quantized outputs are expected to encourage further objective utilization of the products. Such proven usage will then lead to procedures which permit an evaluation of the economic impact of the data.

The programs represent a substantial investment in machine language coding so as to take maximum advantage of computer speed and memory capacity. Even so, projected higher resolution (and possibly color) imaging devices threaten to increase data volumes by one or two orders of magnitude within the next several years. This would likely lead to different applications and different information extraction goals. All of this could saturate today's largest computer and might well indicate the need for the newly projected parallel network computer.

Before that time, experience should provide guidelines for the specification of practical volumes of data to be computer processed commensurate with the application goals. For example, 4-mi. global resolution may suffice for routine monitoring which would guide higher-resolution inspection over automatically selected subregions.

Present experimental products generated from digitized infrared data offer the opportunity of combining descriptors generated from both sources. The eventual data processing task will probably involve the blending of video, infrared, and other indirect sounding data with the increasing variety of direct probe observations. All such data, combined with proper weights and properly adjusted in space and time, will represent a computer task which may rival that represented by the weather prediction problems themselves.

ACKNOWLEDGMENTS

The work herein reported represents more than 15 man-years of program development by a staff of a dozen professionals utilizing skills in mathematics, meteorology, and photogrammetry, and is based upon many more man-years of background experience in satellite data processing. Without providing personal reference, the authors hereby wish to acknowledge the efforts of their co-workers.

REFERENCES[1]

1. R. E. Bradford and R. L. Rossin, "Weather Satellite Picture Calibration," National Environmental Satellite Center (in preparation).
2. R. E. Bradford and J. W. Sears, "An Approach to Automated Nephanalysis," National Environmental Satellite Center (in preparation).
3. C. L. Bristor, "A Summary of Experiences in Computer Processing of Nimbus I Data," *Meteorological Satellite Laboratory Report* No. 27 (in press).
4. C. L. Bristor and W. M. Callicott, "Meteorological Products from Digitized Satellite Vidicon Cloud Pictures," *Meteorological Satellite Laboratory Report* No. 26, U.S. Weather Bureau, January 1964.
5. C. L. Bristor and L. I. Miller, "Processing Satellite Weather Data—A Status Report, Parts I and II," *Proceedings of the 1962 Fall Joint Computer Conference*, Philadelphia, Pa., Dec. 4, 1962.
6. S. Fritz, "The Significance of Mountain Lee Waves as Seen from Satellite Pictures," *Journal of Applied Meteorology*, vol. 4, No. 1, February 1955, pp. 31–37.
7. E. E. Gray and I. F. Davis, "Weather Satellite Digital and Analog Display System," Link Group, General Precision, Inc., Palo Alto, Calif. 1965.
8. R. Hill, "The Digital Format System," National Environmental Satellite Center (in preparation).
9. M. Holl, "Objective Assembly of Meteorological Satellite Information," Navy Contract N62306–1775, Project FAMOS, U.S. Fleet Weather Central, Washington, D.C., July 1966.
10. R. E. Mach and T. L. Gardner, "Rectification of Satellite Photography by Digital Techniques," *IBM Journal of Research and Development*, vol. 6, No. 3, July 1962, pp. 290–305.
11. W. A. Marggraf, "Automatic Data Processing of Weather Satellite Data," *AFCRL–TDR–63–243*, Air Force Cambridge Research Laboratory, Bedford, Mass., Jan. 1963.
12. Sh. A. Mussayelyan, "Some Aspects of the Interpretation and Use of Cloud Data Obtained with Meteorological Satellites," Translation from original Russian, issued by U.S. Office of Technical Services, as Technical Translation TT65–33206, Nov. 1965.
13. Radio Corporation of America, Astro-Electronics Div., "Alignment and Calibration Data for the TIROS IX Meteorological Satellite," *RCA/AED, R–2538*, Nov. 1964.
14. A. H. Thompson, "The Mean Relative Humidity Between the Surface and 500 MB Level Over the Gulf of Mexico," *Final report on contract CWB 11247*, July 1966.
15. A. Wachtel, "Data Acquisition and Processing System for the Nimbus Meteorological Satellite," *National Telemetering Conference*, Albuquerque, N. Mex., May 1963.

[1] Despite its limited availability, certain reference material is listed for those computer-oriented readers who may wish to pursue some of the subject matter in greater detail.

[Received May 5, 1966; revised June 17, 1966]